Damage process of a fiber bundle with a strain gradient

Ferenc Kun[*] and Sándor Nagy

Department of Theoretical Physics, University of Debrecen, P.O. Box 5, H-4010 Debrecen, Hungary
(Received 10 December 2006; revised manuscript received 12 September 2007; published 30 January 2008)

We study the damage process of fiber bundles in a wedge-shape geometry which ensures a constant strain gradient. To obtain the wedge geometry we consider the three-point bending of a bar, which is modeled as two rigid blocks glued together by a thin elastic interface. The interface is discretized by parallel fibers with random failure thresholds, which become elongated when the bar is bent. Analyzing the progressive damage of the system we show that the strain gradient results in a rich spectrum of novel behavior of fiber bundles. We find that for weak disorder an interface crack is formed as a continuous region of failed fibers. Ahead of the crack a process zone develops which proved to shrink with increasing deformation, making the crack tip sharper as the crack advances. For strong disorder, failure of the system occurs as a spatially random sequence of breakings. Damage of the fiber bundle proceeds in bursts whose size distribution shows a power law behavior with a crossover from an exponent 2.5 to 2.0 as the disorder is weakened. The size of the largest burst increases as a power law of the strength of disorder with an exponent $2/3$ and saturates for strongly disordered bundles.

I. INTRODUCTION

The damage and fracture of disordered materials is an important scientific and technological problem which has attracted intensive research during the past years [1–3]. Theoretical and experimental studies have revealed that at the beginning of the loading process of highly disordered materials, first microcracks nucleate randomly, covering the entire volume of the specimen without any spatial correlations [1–4]. Approaching the critical load, localization occurs, resulting in a single growing crack along which the specimen falls apart. In a composite system of two solid blocks glued together along an interface, the damage usually concentrates along the weak plane of the glue [5–8]. Loading such composites, interface crack propagation occurs which has also been found to be a complex sequence of crack growth and arrest with interesting spatial and temporal fluctuations [5–7,9–12]. The crackling noise accompanying the failure of disordered systems (bulk or interface cracking) can be recorded in the form of a complicated trail of signals whose analysis provides important information about the microscopic dynamics of damaging [11,13–18].

Fiber bundle models (FBMs) are one of the most important theoretical approaches to the progressive damage of disordered materials. During the last decade FBMs have provided deep insight into the collective nature of the microscopic dynamics and statistical properties of degradation phenomena. Recently, FBMs have also been applied to study the interfacial failure of glued solid blocks under shear loading [5,8] and wear [6,7,19]. Interesting novel results have been obtained on the temporal and spatial fluctuations of local breakings which precede macroscopic failure and on the analogy of fracture with phase transitions and critical phenomena [5–8,19]. In this paper we study the damage process of a fiber bundle in a wedge-shape geometry, which provides a constant strain gradient of fibers. To obtain a

simple representation of the geometry and loading conditions, we consider a bar subject to three-point bending. The bar is modeled as two rigid blocks coupled together by an elastic interface which is then discretized by a bundle of parallel fibers. Deformation and damage of the bar is concentrated in the interface resulting in a linear deformation profile of fibers, while the two blocks remain intact. Besides interfacial failure, the model provides the mean field limit of the failure of disordered materials under three-point bending. Varying the amount of disorder of fibers, we can control the strength of nonlinearity before macroscopic failure, and hence, the type of fracture (brittle-quasibrittle) of the bundle [15,20,21]. We focus on the progressive damage of the fiber bundle analyzing the damage profile, crack formation, and bursts of local breakings. We find that for weak disorder an interface crack is formed by a continuous region of failed fibers. Ahead of the interface crack, a process zone develops which proved to shrink with increasing deformation making the crack tip sharper. For strong disorder the failure of the bundle occurs due to a spatially random sequence of local breakings. Very interestingly we find that the size distribution of bursts is a power law whose exponent shows a crossover from exponent 2.5 to 2.0 when the strength of disorder is lowered.

We demonstrate that the results of our model calculations are the consequence of the strain gradient; in the homogeneous case of zero gradient, our model recovers all recent results of FBMs with varying threshold disorder [13,15,20,21,27,28]. Our results imply that interfacial fracture problems can lead to novel universality classes of breakdown phenomena.

II. MODEL

In order to obtain a fiber bundle with a linear deformation profile, we construct a simple model for the loading of an elastic bar of rectangular shape by an external force exerted perpendicular to the longer side of the bar in the middle. For simplicity, in the model the bar is composed of two rigid
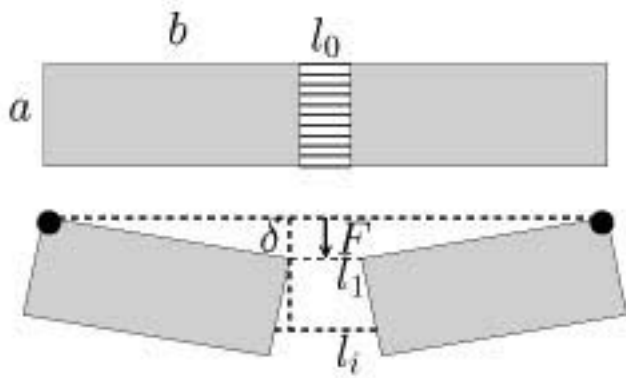
---

*feri@dtp.atomki.hu

FIG. 1. The geometrical layout of the model. The two rigid blocks of side length a and b are glued together by an interface of width l_0 which is discretized in terms of elastic fibers. The specimen suffers deflection δ under the action of the external force F exerted in the middle of the bar. The wedge-shaped opening of the interface results in a linear deformation profile of fibers.

FIG. 2. The constitutive curve $\sigma(\delta)$ of the interface composed of $N=10\,000$ fibers varying the width of the threshold distribution Δ at the fixed value of $\varepsilon_0^c=0.01$. For $\Delta=0$ the constitutive curve $\sigma(\delta)$ has a sharp peak which gets rounded and develops into a quadratic maximum when Δ is increased.

blocks of side lengths a and b which are glued together by an elastic interface of width l_0, where $l_0 \ll b$ holds; see Fig. 1. The interface region can deform and suffer breaking under deflection of the specimen while the two rigid blocks remain intact. Bending of the specimen is performed such that the two blocks undergo rigid rotation about their outer upper corner, concentrating the deformation in the interface layer. We discretize the interface in terms of elastic fibers of number N and length l_0 which are placed equidistantly between the two blocks. The fibers do not have bending rigidity; they can undergo only stretching deformation characterized by the same value of the Young modulus E. During the bending of the specimen, the fibers can support only a finite deformation, i.e., if the local deformation ε_i of fiber i exceeds a threshold value ε_i^c the fiber breaks and a microcrack nucleates in the interface. The disordered properties of the material are represented by the randomness of the breaking thresholds ε_i^c, which are independent identically distributed random variables with a probability density $p(\varepsilon)$ and cumulative distribution $P(\varepsilon^c) = \int_0^{\varepsilon^c} p(x)dx$. The rigidity of the two rotating blocks implies that the macroscopic deformation of the specimen can be characterized by a single variable δ which denotes the deflection of the middle of the bar from the original position; see Fig. 1.

It can be seen in Fig. 1 that under bending of the specimen the interface opens, resulting in an increasing elongation of fibers from top to bottom. The actual length of fibers l_i can be expressed as a function of δ as

$$l_i = l_1 + 2\delta \frac{a}{b} \frac{i-1}{N-1}, \quad i=1,\dots,N, \qquad (1)$$

where $l_1 = l_0 + 2(b - \sqrt{b^2 - \delta^2})$ is the length of fiber index $i=1$ at the top of the bar. It follows that also the elongation Δl_i and longitudinal strain ε_i of fibers increase linearly as a function of their position i:
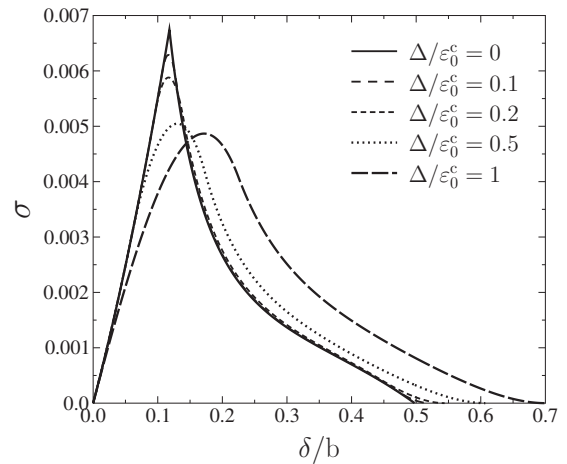
$$\Delta l_i = 2b - 2\sqrt{b^2 - \delta^2} + 2\delta \frac{a}{b} \frac{i-1}{N-1}, \qquad (2)$$

$$\varepsilon_i = \frac{\Delta l_i}{l_0}. \qquad (3)$$

Equilibrium of the system is obtained when the total momentum of forces with respect to the clamping points is zero. During the deformation process, those fibers which exceed their threshold value break; i.e., they are removed from the interface. Since $1 - P(\varepsilon_i(\delta))$ is the probability that the interface element of index i remained intact under the externally imposed deformation δ, based on the equilibrium condition, the constitutive equation $\sigma(\delta)$ of the deflected bar can be cast in the form

$$\sigma(\delta) = \frac{1}{NL} \sum_{i=1}^{N} \left[\delta + \sqrt{b^2 - \delta^2} \frac{a}{b} \frac{(i-1)}{(N-1)} \right]$$
$$\times [1 - P(\varepsilon_i(\delta))] E \varepsilon_i(\delta), \qquad (4)$$

where $L = 2b + l_0$ is the overall length of the bar and the sum goes over all the fibers. On the right-hand side $\varepsilon_i(\delta)$ should be substituted from Eqs. (2) and (3). The above equations describe the macroscopic response of a fiber bundle which has a linear deformation profile. In the following, for the explicit calculations the geometrical parameters were set as $a=1$, $b=2.5$, and $l_0=0.1$.

The amount of disorder of the failure thresholds ε_i^c has a substantial effect on the macroscopic response of the fiber bundle $\sigma(\delta)$. In the limiting case of zero disorder—i.e., when all the fibers have the same breaking threshold $\varepsilon_i^c = \varepsilon_0^c$—the failure of the bundle starts at the bottom of the interface where the stretching deformation is the highest and proceeds upward as δ is increased. It can be seen in Fig. 2 that the corresponding constitutive curve is sharply peaked. The critical deformation δ_c defined by the peak position correspond

to the instant of the first fiber breaking $\varepsilon_0^c = \varepsilon_N(\delta_c)$. Beyond the peak stress, σ rapidly decreases due to the gradual breaking of fibers as δ increases. In order to study how the behavior of the system changes when the amount of disorder of fibers is varied, we consider a uniform distribution for the breaking thresholds over an interval of width 2Δ centered at the value ε_0^c:

$$P(\varepsilon^c) = \frac{\varepsilon^c - (\varepsilon_0^c - \Delta)}{2\Delta}, \quad \varepsilon_0^c - \Delta < \varepsilon^c < \varepsilon_0^c + \Delta. \quad (5)$$

The strength of disorder of the breaking thresholds is characterized by Δ, while ε_0^c sets the scale of fiber strength. The width Δ can be varied over the interval $[0, \varepsilon_0^c]$ where the limits $\Delta = 0$ and $\Delta = \varepsilon_0^c$ corresponds to zero disorder and the strongest disorder, respectively. Figure 2 shows that increasing Δ, the peak of the constitutive curve gets more and more rounded and develops into a quadratic maximum. The maximum of $\sigma(\delta)$ is preceded by a longer and longer nonlinear regime due to the breaking of fibers, so that for $\Delta \to \varepsilon_0^c$ the linear behavior prevails only for small deformations $\delta \to 0$. On the microlevel this process is accompanied by the randomization of the breaking sequence of fibers along the interface, i.e., for $\Delta \neq 0$, fibers do not simply break in the decreasing order of their index i (from bottom to top of the bar).

III. SIMULATION TECHNIQUES

The complete constitutive curve of the system presented in Fig. 2 can only be recovered by deformation-controlled loading. When δ is controlled externally, the local load on the fibers is solely determined by the externally imposed deformation, so that there is no load redistribution after fiber breaking. Under stress-controlled conditions, the breaking of fibers is followed by the redistribution of load over the intact ones. Due to the wedge shape of the deformed interface, at a given external load σ, the load on the fibers linearly increases from top to bottom. It has the consequence that in spite of the rigidity of the two solid blocks, the load redistribution following fiber failure differs from the usual equal load sharing (ELS) approximation commonly used for the study of parallel bundles of fibers [2,4,20,22,23]. The rigid surfaces, however, ensure that the load is redistributed globally in such a way that the excess load received by an intact fiber depends on its position along the interface but not on its distance from the failed one. This implies that no stress enhancement arises in the vicinity of the failed fibers as in the case of the local load sharing approximation (LLS) of fiber bundles [2,21,24]. Our fiber bundle model provides the mean-field limit of the damage and fracture of disordered materials under three-point bending conditions and also represents an interesting interface rupture problem.

In order to analyze the microscopic damage mechanism of FBMs with a constant strain gradient, we worked out an efficient simulation technique for a sample where the interface is composed of N fibers with breaking thresholds ε_i^c, $i = 1, \dots, N$, sampled from the probability distribution, Eq. (5). Substituting the breaking thresholds ε_i^c on the left-hand side

of Eq. (2) and inverting it for δ, we can determine the value of the macroscopic deformation parameter $\delta_i^c = \delta(\varepsilon_i^c, i)$, $i = 1, \dots, N$, at which the fibers break. Of course, δ_i^c is a function of both the position of the fiber i along the interface and the local breaking threshold ε_i^c. During the loading process the fibers break in the increasing order of their critical macroscopic deformation δ_i^c, which can be a randomized sequence of the fibers' position i. The computer simulation of the loading process proceeds as follows: after generating the breaking thresholds of fibers ε_i^c we determine the corresponding critical deflections δ_i^c and sort them into increasing order. The constitutive curve of the sample can be simply obtained by calculating the load needed to achieve the deformation δ_i^c after the breaking of the first $i-1$ fiber with there remaining only $N_{intact} = N - (i-1)$ intact elements. Between the breaking of the $(i-1)$th and ith fibers, the constitutive equation of the system takes the form

$$\sigma = \frac{E}{l_0 L} \left\{ 2\delta[b - \sqrt{b^2 - \delta^2}]N_{intact} \right.$$
$$+ \left[\delta^2 \frac{4a}{b} - 2ab + 2a\sqrt{b^2 - \delta^2} \right] \frac{1}{N-1} \sum_{j=1}^{N}{}'(j-1)$$
$$\left. + \frac{2\delta a^2}{(N-1)^2 b^2} \sqrt{b^2 - \delta^2} \sum_{j=1}^{N}{}'(j-1)^2 \right\}, \quad (6)$$

where the prime indicates that the summation is restricted to indices of intact fibers (which are not necessarily consecutive integers). Note that in Eq. (6) the value of δ falls in the range $\delta_{i-1}^c < \delta < \delta_i^c$.

Performing stress-controlled experiments, after the breaking of a fiber the deformation of the specimen can freely change, resulting in a redistribution of load over the intact fibers. The excess load taken up by the intact fibers can give rise to further fiber failures which may trigger an entire avalanche of breakings. This avalanche either stops and the bar becomes stable under the externally imposed load or it spans the entire interface and the specimen breaks into two pieces (the entire bundle ruptures). In order to study numerically this microscopic breaking process, in the simulations first we increase the deformation δ such that a single fiber breaks—i.e., $\delta = \delta_1^c$ with index i_1. Then the load needed to maintain this deformation σ is calculated from Eq. (6) for $N_{intact} = N$ fibers. After the breaking of fiber i_1 its load has to be redistributed over the remaining $N-1$ fibers. In order to determine the load of intact fibers after the removal of the broken one, we remove fiber i_1 on the right-hand side of Eq. (6) and invert the equation for $\delta(\sigma)$, keeping the load σ fixed. The fibers with threshold values $\delta_i^c < \delta(\sigma)$ break as a consequence of the load redistribution. This iteration has to be repeated under a fixed external load σ until the breaking sequence stops or all the fibers break, resulting in a macroscopic failure of the system.

IV. SPATIAL EVOLUTION OF DAMAGE

In a bundle of fibers loaded between two parallel rigid plates, due to the equal load sharing after fiber breaking, the
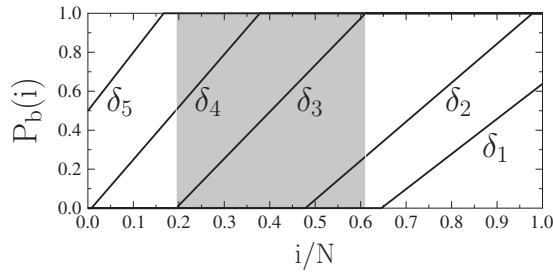
FIG. 3. Damage profile—i.e., the breaking probability P_b of fibers along the interface at five different values of the deflection $\delta_1 < \delta_2 < \delta_3 < \delta_4 < \delta_5$ with $\Delta/\varepsilon_0^c = 0.2$ and $b/a = 2.5$. The deflection δ_1 falls in regime (A), $\delta_2, \delta_3, \delta_4$ are in (B), and δ_5 belongs to (C). The increase of the slope of the straight lines indicates the sharpening of the profile. The shadowed area highlights the process zone for δ_3.

failure of a fiber is solely determined by its breaking threshold [13–15,25]. Hence, fibers break in a completely random sequence without any spatial correlations. In our system, however, during the loading process the fibers break in increasing order of their critical macroscopic deformation $\delta_i^c(\varepsilon_i^c, i)$, which depends both on the local breaking thresholds ε_i^c and on the spatial position i of fibers. In the limiting case of zero disorder—i.e., $\Delta = 0$ and $\varepsilon_i^c = \varepsilon_0^c$—the critical deformation $\delta_i^c(\varepsilon_0^c, i)$ is a monotonically decreasing function of i, which implies that the fibers break one by one starting from the bottom. This breaking sequence can be conceived as a crack which is generated and penetrates the interface upward such that below the crack tip all the fibers are broken while above it the fibers are intact. Under strain-controlled loading stable crack propagation is obtained, gradually breaking the fibers by the strain increments. Controlling the external load, however, the onset of crack propagation occurs in an unstable manner, resulting in immediate catastrophic failure when the maximum of $\sigma(\delta)$ is reached (see Fig. 2).

Increasing the strength of disorder Δ, the breaking sequence of fibers determined by δ_i^c becomes spatially randomized. At a given deformation δ, the fibers with $\delta_i^c < \delta$ have already failed. If the disorder is not too strong, an interesting spatial distribution of these broken fibers emerges: starting from the bottom of the interface a continuous region of failed fibers develops, forming a crack. On the opposite side, starting from the top of the interface a continuous region of intact, elongated fibers can be observed. The two regimes are separated by a process zone, which is a sparse sequence of intact and broken elements. To illustrate this feature, in Fig. 3 we show the probability $P_b(i)$ that the fibers are broken along the interface for several different values of δ using the threshold distribution, Eq. (5). The probability $P_b(i)$ that fiber i is broken at the deflection δ can be obtained directly from the threshold distribution $P_b(i) = P(\varepsilon_i(\delta))$. The process zone is defined as the regime where for the probability P_b of fiber breaking $0 < P_b < 1$ holds. It can be observed in Fig. 3 that the process zone sharpens, i.e., its width decreases as the deformation δ increases which makes the crack tip sharper as the crack advances. It can be obtained analytically that at a given deflection δ the width W of the process zone depends
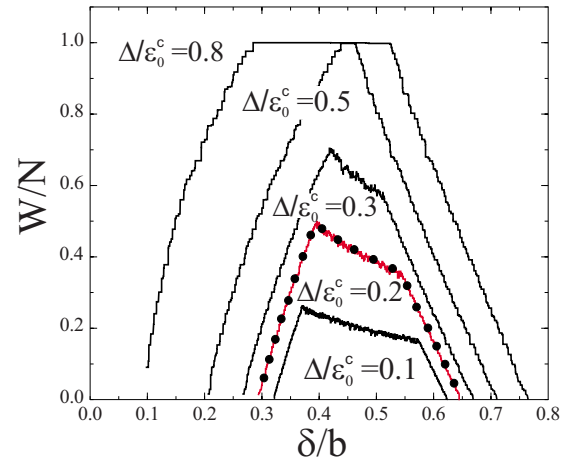

FIG. 4. (Color online) Width of the process zone, W/N, as a function of the deflection δ of the bar for several values of Δ. Computer simulations are in perfect agreement with the analytic predictions, Eqs. (7)–(9), represented by the dots for the specific case of $\Delta/\varepsilon_0^c = 0.2$.

both on the strength of disorder Δ and on the geometrical extensions a and b of the specimen. For the explicit calculations, it is worth considering separately the following three regimes of the damage profile: (A) for the breaking probability at the bottom of the interface it holds that $P_b(i=N) < 1$—i.e., the crack has not yet developed (δ_1 in Fig. 3); (B) the process zone is completely contained by the interface $P_b(i=1) = 0$ and $P_b(i=N) = 1$ ($\delta_2, \delta_3, \delta_4$ in Fig. 3); and (C) there is no intact region $P_b(i=1) > 0$ (δ_5 in Fig. 3). The width W of the process zone can be obtained analytically as a function of δ for the three cases

$$(A) \quad W = N \left[1 - \frac{\varepsilon_0^c - \Delta - 2b + 2\sqrt{b^2 - \delta^2}}{2\delta} \frac{b}{a} \right], \quad (7)$$

$$(B) \quad W = \frac{\Delta}{\delta} \frac{b}{a} (N - 1), \quad (8)$$

$$(C) \quad W = N \frac{\varepsilon_0^c + \Delta - 2b + 2\sqrt{b^2 - \delta^2}}{2\delta} \frac{b}{a}. \quad (9)$$

We also determined the width of the process zone, W, numerically for a system of 10^6 fibers, which is presented in Fig. 4 together with the corresponding analytic results. In Fig. 4 the curves of $W(\delta)$ are composed of three distinct parts corresponding to regimes (A), (B), and (C) of Eqs. (7)–(9). It can be seen that for smaller values of Δ/ε_0^c first W increases and reaches a maximum where the crack occurs. As the crack advances, the width of the process zone decreases according to Eq. (8) and finally, as the tip of the process zone reaches the top of the interface, W rapidly decreases as given by Eq. (9). It is interesting to note that for large Δ values no crack can be identified, i.e., for the parameter set used in Fig. 4 the damage profile spans the entire interface $\max[W/N] = 1$ when Δ/ε_0^c exceeds 0.46. It follows from the above arguments that the disorder of the interface can be considered strong if the
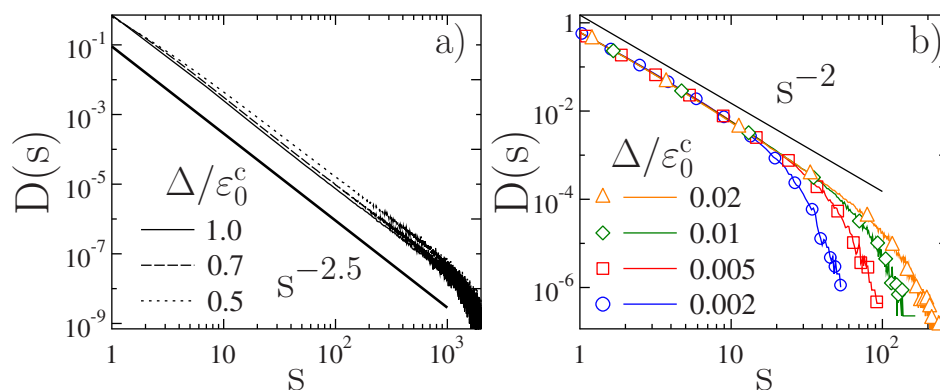
FIG. 5. (Color online) (a) Distribution of burst sizes $D(s)$, varying the value of Δ in a broad range. (b) Distributions for the limiting case of very weak disorder. Simulations were carried out with $N=10^6$ fibers averaging over 10^3 samples. The geometrical layout of the sample was $b/a=2.5$, and the scale parameter of fibers' strength had the value $\varepsilon_0^c=0.01$. Straight lines of slope 2.5 and 2.0 are drawn as reference.

damage proceeds as a spatially random sequence of local breakings without the formation of a propagating crack. No crack can develop if at the deformation δ where the top of the interface may already be damaged $\varepsilon_1(\delta) > \varepsilon_0^c - \Delta$ the bottom of the interface may still be intact $\varepsilon_N(\delta) < \varepsilon_0^c + \Delta$. Making use of Eq. (2) and assuming $b \gg \varepsilon_0^c - \Delta$, the condition of strong disorder can be formulated as

$$\frac{b}{a^2}\Delta^2 + \Delta > \varepsilon_0^c, \qquad (10)$$

which implies that the average fiber strength ε_0^c, the width of the distribution Δ, and the geometrical layout a and b of the specimen together determine the relevance of disorder. At a given value of a, b, and ε_0^c, the crossover point Δ^* between weak and strong disorder can be obtained as

$$\Delta^* \approx \frac{a^2}{2b}\left[\sqrt{1 + \frac{4b\varepsilon_0^c}{a^2}} - 1\right], \qquad (11)$$

so that for $\Delta > \Delta^*$ no crack is formed, while for $\Delta < \Delta^*$ crack propagation occurs with a shrinking process zone ahead f the crack tip. For the parameter values of Fig. 4 the crossover point $\Delta^*=0.4633$ was obtained from Eq. (11), in excellent agreement with the numerical results.

V. BURSTS OF FIBER BREAKINGS

In order to characterize the damage process of the fiber bundle under stress-controlled conditions, we determined the distribution of burst sizes s of fiber breakings varying the width Δ of the disorder distribution. Simulations were carried out by increasing the external load to break a single fiber and following the cascading fiber breakings with the algorithm discussed in Sec. III. The avalanche size distributions $D(s)$ are presented in Fig. 5, varying the amount of disorder in a broad range. It can be observed in Fig. 5 that $D(s)$ has a power law form

$$D(s) \sim s^{-\tau} \qquad (12)$$

at any finite value of Δ with an exponential cutoff at large avalanches. Simulations revealed an interesting change of

the value of the exponent τ as the strength of disorder is varied: for strong disorder the value of τ coincides with the mean-field (equal load sharing) exponent of the classical parallel bundle of fibers $\tau \approx 2.5$ [13,26]. However, as the disorder is weakened, the distribution exhibits a crossover to another power law with a lower exponent $\tau \approx 2.0$. To better illustrate this effect, in Fig. 5(b) burst distributions are shown separately for the limiting case of very weak disorder. The numerical results are well described by a power law with an exponent 2.0.

It is interesting to note that the size of the largest burst s_{max} has a strong dependence on the value of Δ [see Fig. 5(b)]; namely, as the strength of disorder is reduced, the largest avalanche decreases. To obtain a quantitative characterization of this effect, Fig. 6 presents the average size of the largest bursts $\langle s_{max} \rangle$ as a function of Δ, where a power law dependence is evidenced,

$$\langle s_{max} \rangle \sim \Delta^\alpha, \qquad (13)$$

for the case of weak disorder $\Delta < \Delta^*$. As Δ exceeds Δ^*, the largest avalanche s_{max} reaches a maximum and levels off (see
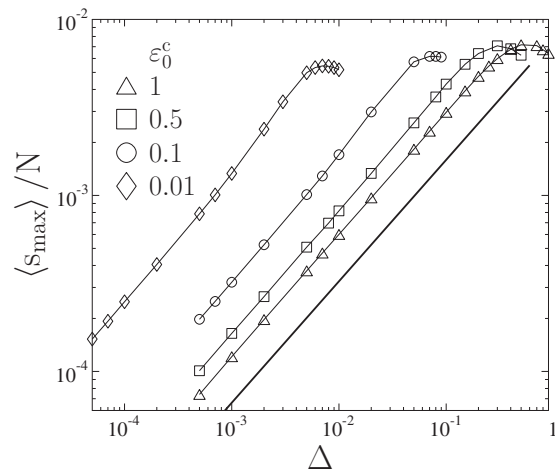

FIG. 6. Average size of the largest avalanche as a function of Δ for several values of ε_0^c. A straight line of slope 2/3 is drawn to guide the eye.
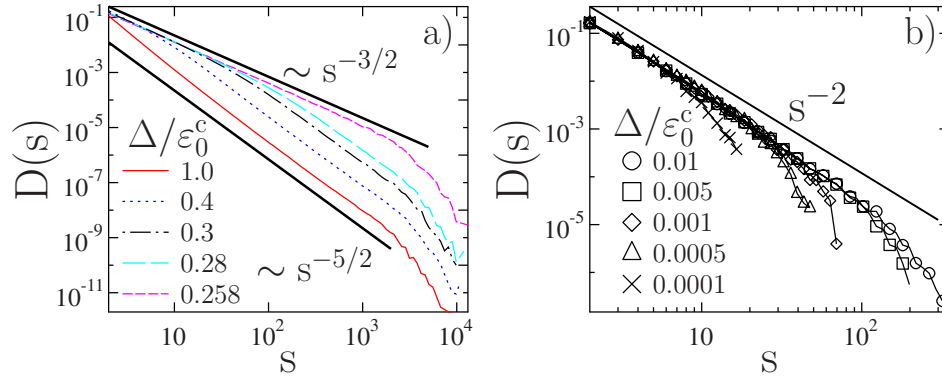
FIG. 7. (Color online) (a) Burst size distributions for the limiting case of zero strain gradient ($a=0.0$). There exists a finite critical disorder $\Delta_c \approx 0.258$, where a crossover occurs from the exponent $5/2$ to a lower value $3/2$. (b) At any finite value of $a > 0$ criticality is obtained only for $\Delta \rightarrow 0$ and the crossover exponent becomes larger.

Fig. 6). Computer simulations revealed that the exponent α has a universal value $\alpha = 2/3$ indicated by the straight line drawn in Fig. 6 to guide the eye. The value of Δ where $\langle s_{max} \rangle$ saturates is in good agreement with the corresponding value of Δ^* estimated from Eq. (11).

It is important to emphasize that in our system no critical disorder distribution can be identified in the sense defined in Refs. [15,21,27–30]. For equal-load-sharing fiber bundles the threshold distribution is considered to be critical if the breaking of the weakest fiber gives rise to an immediate macroscopic failure of the system. For uniformly distributed threshold values in the interval $[x_0, 1]$ the distribution becomes critical for $x_0 \rightarrow 0.5$ [15,21,27–30]. It has been pointed out that approaching the critical disorder, the macroscopic response of the system becomes perfectly brittle and on the microlevel the size distribution of bursts exhibits a crossover from a power law of exponent 2.5 to a significantly lower one 1.5 [15,21]. Using our terminology, such critical behavior in a bundle of fibers loaded between two parallel rigid plates—i.e., in the case of equal load sharing—should be obtained for $\Delta \rightarrow \varepsilon_0^c/3$; however, computer simulations revealed a sudden collapse of our FBM with constant strain gradient solely at $\Delta = 0$.

The reason for the missing critical state in our model is the inhomogeneity of the load of fibers along the interface. Equation (2) shows that at any deflection δ the load of intact fibers linearly increases from top to bottom of the interface where the gradient—i.e., the strength of inhomogeneity—is determined by the geometry of the system, a/b. Setting the cross section of the specimen a to zero, $a=0$, the positional dependence of ε_i disappears in Eqs. (2)–(4) and formally all the fibers keep the same load determined by δ. We carried out computer simulations in the limiting case $a=0$, varying the strength of disorder Δ. We indeed find that in this homogeneous case a critical state arises at $\Delta_c/\varepsilon_0^c \approx 0.258$ such that for $\Delta < \Delta_c$ a single fiber breaking triggers a catastrophic avalanche. The corresponding numerical results are presented in Fig. 7(a), where it can be seen that approaching Δ_c from above, the burst size distribution exhibits a crossover from the exponent $\tau = 5/2$ to a lower value $\tau = 3/2$, in agreement with the predictions of Refs. [15,27,28]. The deviation of Δ_c from $\varepsilon_0^c/3$ arises due to the nonlinear terms of δ in Eqs. (2)

and (4). It can also be observed in the figure that in the homogeneous case the largest burst s_{max} increases as criticality is approached in agreement with Ref. [21].

However, at any finite value of a—i.e., in the presence of a strain gradient—the picture drastically changes: criticality occurs solely in the limit $\Delta \rightarrow 0$ so that catastrophic failure is always preceded by avalanches with a power law distribution but the cutoff avalanche size goes to zero as a power law of Δ when Δ is decreased. Figure 7(b) presents simulation results obtained with 10^6 fibers at the value $a=0.01$, which results in a much lower strain gradient than in Fig. 5. Comparing the burst size distributions of different values of Δ for the homogeneous [Fig. 7(a)] and inhomogeneous [Fig. 7(b)] cases, a clear difference can be observed. The higher value of the crossover exponent $\tau = 2$ compared to $\tau = 3/2$ of the homogeneous case shows that in the absence of a finite critical disorder, the large avalanches are less dominating in the distributions $D(s)$.

VI. DISCUSSION

We presented a detailed study of the progressive damage and fracture of fiber bundles in a wedge-shape geometry which provides a linear deformation profile for fibers. For a simple representation of the geometrical and loading conditions of the system, we considered a bar subjected to three-point bending. The bar is composed of two rigid blocks coupled by an elastic interface which is then discretized in terms of parallel fibers. We showed that in the limit of zero disorder of fibers' strength the bundle has a perfectly brittle macroscopic response, i.e., under stress-controlled loading, global failure occurs as a sudden collapse of the system without any precursory activity. Furthermore, fibers break in a completely ordered sequence from bottom to top of the wedge, creating an unstable crack with a sharp tip. The relevance of disorder is determined together by the parameters (mean and width) of the strength distribution of fibers and by the geometrical layout of the wedge. We demonstrated that a propagating interface crack can only be defined for weak disorder. Ahead of the crack a process zone is formed whose width decreases with increasing deformation making the crack tip sharper as the crack advances. For strong disorder a

spatially random sequence of local breakings occurs along the entire bundle.

The breaking of single fibers can trigger cascades of breaking events. The size distribution of these bursts is found to be a power law with an interesting crossover effect as the strength of disorder is varied: for strong disorder the mean-field exponent $\tau = 5/2$ of equal-load-sharing fiber bundles is recovered indicating the complete randomness of the failure process. However, for weak disorder where a propagating crack with a process zone develops, a lower exponent $\tau = 2.0$ is obtained. In the weak disorder regime the largest burst increases as a power law of the width of the disorder distribution with an exponent $\alpha = 2/3$. We showed that in the limit of zero strain gradient our calculations reproduce the crossover of burst exponents from $5/2$ to $3/2$ predicted recently. The features of our system originate from the finite strain gradient—i.e., from the geometrical constraints of fibers which naturally occur, for instance, at interfacial fracture problems. Our model provides also the mean-field limit of the damage and fracture of disordered materials under three-point bending. The results imply that the statistical physics of interfacial rupture can reveal universality classes of breakdown phenomena.

Recently, it was found experimentally that the cracking of a bar under three-point bending proceeds in bursts which are characterized by power law distributions [31]. The experiments showed that the exponents of the amplitude, area, and energy distribution of magnetic emission signals recorded during the fracture process of ferromagnetic materials are sensitive to the type of fracture; i.e., the noise spectra of ductile materials are characterized by higher exponents than the brittle ones. The boundary and loading conditions ensured in the experiments that the damage localizes to a relatively thin layer of the specimen, giving rise to a single growing crack so that the crackling noise measured during the loading process characterizes the crack propagation. Note that in our model the crossover to a lower exponent of burst sizes with decreasing disorder is accompanied on the macrolevel by an increasing degree of brittleness showing that this simple mean-field approach can qualitatively account for the changing properties of crackling noise observed experimentally [31].

[1] B. K. Chakrabarti and L. G. Benguigui, *Statistical Physics of Fracture and Breakdown in Disordered Systems* (Oxford University Press, Oxford, 1997).

[2] M. Alava, P. K. Nukala, and S. Zapperi, Adv. Phys. **55**, 349 (2006).

[3] *Statistical Models for the Fracture of Disordered Media*, edited by H. J. Herrmann and S. Roux (Elsevier, Amsterdam, 1990).

[4] F. Kun, F. Raischel, R. C. Hidalgo, and H. J. Herrmann, in *Modelling Critical and Catastrophic Phenomena in Geoscience: A Statistical Physics Approach*, edited by P. Bhattacharyya and B. K. Chakrabarti, Lecture Notes in Physics, (Springer-Verlag, Berlin, 2006), Vol. 705, pp. 57–92.

[5] F. Raischel, F. Kun, and H. J. Herrmann, Phys. Rev. E **72**, 046126 (2005).

[6] A. Delaplace, S. Roux, and G. Pijaudier-Cabot, Int. J. Solids Struct. **36**, 1403 (1999).

[7] J. Knudsen and A. R. Massih, Phys. Rev. E **72**, 036129 (2005).

[8] F. Raischel, F. Kun, and H. J. Herrmann, Phys. Rev. E **73**, 066101 (2006).

[9] G. G. Batrouni, A. Hansen, and J. Schmittbuhl, Phys. Rev. E **65**, 036126 (2002).

[10] S. Roux, A. Delaplace, and G. Pijaudier-Cabot, Physica A **270**, 35 (1999).

[11] K. J. Maloy, S. Santucci, J. Schmittbuhl, and R. Toussaint, Phys. Rev. Lett. **96**, 045501 (2006).

[12] L. Salminen, J. M. Pulakka, J. Rosti, M. Alava, and K. Niskanen, Europhys. Lett. **73**, 55 (2006).

[13] M. Kloster, A. Hansen, and P. C. Hemmer, Phys. Rev. E **56**, 2615 (1997).

[14] A. Hansen and P. C. Hemmer, Phys. Lett. A **184**, 394 (1994).

[15] S. Pradhan, A. Hansen, and P. C. Hemmer, Phys. Rev. Lett. **95**, 125501 (2005).

[16] A. Garcimartín, A. Guarino, L. Bellon, and S. Ciliberto, Phys. Rev. Lett. **79**, 3202 (1997).

[17] A. Guarino, A. Garcimartin, and S. Ciliberto, Eur. Phys. J. B **6**, 13 (1998).

[18] L. I. Salminen, A. I. Tolvanen, and M. J. Alava, Phys. Rev. Lett. **89**, 185503 (2002).

[19] A. Delaplace, S. Roux, and G. Pijaudier-Cabot, J. Eng. Mech. **127**, 646 (2001).

[20] J. V. Andersen, D. Sornette, and K. T. Leung, Phys. Rev. Lett. **78**, 2140 (1997).

[21] F. Raischel, F. Kun, and H. J. Herrmann, Phys. Rev. E **74**, 035104(R) (2006).

[22] P. Bhattacharyya, S. Pradhan, and B. K. Chakrabarti, Phys. Rev. E **67**, 046122 (2003).

[23] F. Kun, S. Zapperi, and H. J. Herrmann, Eur. Phys. J. B **17**, 269 (2000).

[24] R. C. Hidalgo, Y. Moreno, F. Kun, and H. J. Herrmann, Phys. Rev. E **65**, 046148 (2002).

[25] R. C. Hidalgo, F. Kun, and H. J. Herrmann, Phys. Rev. E **64**, 066122 (2001).

[26] P. C. Hemmer and A. Hansen, J. Appl. Mech. **59**, 909 (1992).

[27] S. Pradhan and A. Hansen, Phys. Rev. E **72**, 026111 (2005).

[28] S. Pradhan, A. Hansen, and P. C. Hemmer, Phys. Rev. E **74**, 016122 (2006).

[29] U. Divakaran and A. Dutta, Phys. Rev. E **75**, 011117 (2007).

[30] U. Divakaran and A. Dutta, Phys. Rev. E **75**, 011109 (2007).

[31] F. Kun, G. B. Lenkey, N. Takács, and D. L. Beke, Phys. Rev. Lett. **93**, 227204 (2004).